Fluid-Mineral Interactions: A Tribute to H. P. Eugster
© The Geochemical Society, Special Publication No. 2, 1990
Editors: R. J. Spencer and I-Ming Chou

Clay-carbonate reactions in the Venture area, Scotian Shelf, Nova Scotia, Canada

IAN HUTCHEON
Department of Geology and Geophysics, The University of Calgary, Calgary, Alberta, T2N 1N4 Canada

Abstract—The sandstones of the over pressured zone of the Venture Field at 4500 m depth show abundant authigenic chlorite that can be interpreted to have formed by a reaction between kaolinite and ankerite. The stability of this mineral reaction in a H_2O-CO_2-NaCl fluid can be determined from mineral compositions, thermodynamic data and the solubility of CO_2 in saline fluids. The predicted equilibrium temperatures are approximately 160°C, which is in good agreement with measured temperatures. The measurement of ^{13}C for CO_2 and calcite in the gas shows many samples to be in isotopic equilibrium at reservoir temperature, providing additional evidence that the CO_2 in the gas was derived from calcite dissolution.

The reaction mechanism that produces CO_2 in this and other sedimentary basins and in geothermal wells is not defined by the equilibrium treatment of the stability of clay carbonate reactions. However examination of temperature-pCO_2 trends reported by other authors suggests that silicate hydrolysis may be the source of hydrogen ions that cause calcite dissolution. This hypothesis can be tested by examining representative fluid compositions and imposing equilibrium with the appropriate mineral assemblage to determine the value of pCO_2 in equilibrium with silicates and carbonates. Calculated values for pCO_2 for quartzose sediments containing kaolinite, illite and calcite, used to model pCO_2 trends in the Gulf Coast, show good agreement with observed data. Reactions with albite, calcite and analcime, used to model pCO_2 trends in Iceland, do not show as reasonable agreement with measured trends of pCO_2. While not demonstrating unequivocally that CO_2 at deeper levels in sedimentary basins results from dissolution of carbonates, driven by silicate hydrolysis, the evidence to support this hypothesis is strong.

INTRODUCTION

CARBON DIOXIDE is present in natural gases in many sedimentary basins. Studies of the Gulf Coast and North Sea (LUNDEGARD *et al.*, 1984; LUNDEGARD and LAND, 1986; SMITH and EHRENBERG, 1989) have shown that the partial pressure of CO_2 increases with increasing temperature and, therefore, depth. The continuous increase observed in these two basins suggests that the process responsible for the accumulation of CO_2 at greater depths is progressive and HUTCHEON and ABERCROMBIE (1989a), by considering the analyses of produced waters from steam flood pilots, have suggested that the hydrolysis of silicates produces hydrogen ions which are consumed by the dissolution of calcite, releasing CO_2. HUTCHEON *et al.* (1990) have shown that the isotopic composition of CO_2, generated in steam flood pilots, is consistent with an origin from dissolution of calcite. In the Venture Field, there is evidence for the reaction between clays and carbonates and the purpose of this paper is: to describe the conditions under which this reaction might have occurred; to present some supporting isotopic evidence for carbonates being the source of CO_2; and to propose a reaction mechanism that will produce CO_2 and adequately describe the pCO_2-temperature relationships noted by SMITH and EHRENBERG (1989).

The potential for reactions between clay minerals and carbonates during late diagenesis and low grade metamorphism was recognized by ZEN (1959). The reaction of kaolinite and dolomite (or ankerite) to form chlorite was described in the Salton Sea hydrothermal system by MUFFLER and WHITE (1969). Reactions between silicates and carbonate to produce CO_2 have been proposed by HUTCHEON *et al.* (1980), MCDOWELL and PACES (1985) and SMITH and EHRENBERG (1989). HUTCHEON *et al.* (1980) described the potential of univariant reactions between silicates and carbonates to buffer the CO_2 content of an aqueous fluid to the solubility surface between H_2O and CO_2 and, potentially, to produce a CO_2-rich vapour once the solubility surface was reached; however, a reaction mechanism was not proposed. For a fluid containing only H_2O and CO_2, and using pure magnesium end-member chlorite (clinochlore), dolomite and calcite, they calculated the intersection between the kaolinite-dolomite-chlorite mineral reaction and the solubility surface to be at approximately 200°C at 100 MPa (1 Kbar). In general, mineral reactions during diagenesis and low grade metamorphism take place in a saline aqueous fluid and the minerals are not pure end-members. To produce applicable estimates of the stability of the kaolinite-dolomite-chlorite reaction relative to the H_2O-CO_2 miscibility surface, the cal-

culations should incorporate the effect of NaCl on the solubility of CO_2 and the effect of variations in the chemical compositions of chlorite and carbonates.

In this paper, evidence is presented for the reaction of kaolinite and ankerite (or dolomite) to produce chlorite, iron-bearing calcite and CO_2 in the Venture area of the Scotian Shelf (Fig. 1). Data from natural gas wells have been used for estimates of fluid salinity and electron microprobe analyses have provided the composition of the minerals. The stability of chlorite, relative to the H_2O-CO_2 solubility surface in an NaCl-bearing fluid, has been calculated from these compositions and thermochemical data. The possibility that reactions between silicates and carbonates may be a source of CO_2 is examined using the isotopic compositions of the carbonates and CO_2.

The Venture area is an ideal location to examine mineral reactions during diagenesis at higher temperatures. Gas is contained in highly over pressured sandstones (up to 120 MPa) of the Missisauga Formation and temperatures may be in excess of 160°C, depending on the depth. The formation fluids are saline (approximately 20 wt. percent NaCl equivalent) and the gas contains CH_4 and CO_2. Drilling for natural gas in the area has provided rock samples from cored boreholes, water salinities and gas samples for compositional and isotopic analyses.

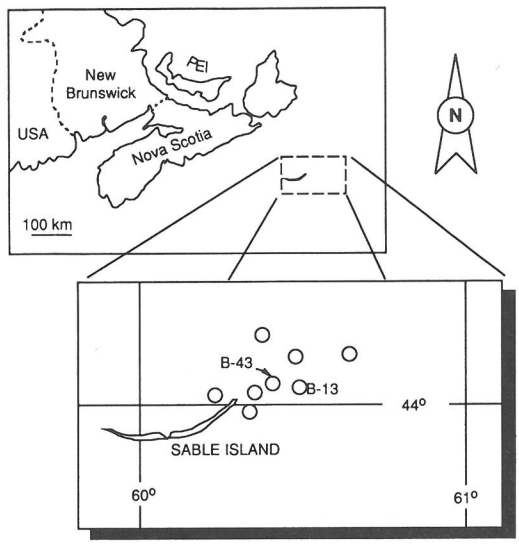

FIG. 1. General location map showing the position of the Venture field relative to the Eastern Coast of Canada and the locations of wells from which rock and fluid samples were obtained in this study.

GEOLOGICAL SETTING

The locations of wells studied are shown in Fig. 1. Not all wells have been cored and most of the samples discussed in this paper are from the Missisauga Formation and were obtained from Venture B-13, B-43, H-22 and B-52, Arcadia J-16, Olympia A-12, Citnalta I-59, Bluenose G-47 and 47A, South Venture O-59, West Venture C-62 and Thebaud I-93.

The stratigraphy of the Scotian Shelf was first presented by MCIVER (1972) and modified by GIVEN (1977). Biostratigraphy was presented by GRADSTEIN *et al.* (1975). The study by GIVEN (1977) incorporated lithofacies descriptions (PIPER, 1975; SWIFT *et al.*, 1975) and paleogeographic and structural studies (HAWORTH, 1975; PARSONS, 1975; HOWIE and BARSS, 1975; JANSA and WADE, 1975; SMITH, 1975). KEEN (1979, 1983) and KEEN and LEWIS (1982) delineated potential zones of organic maturity on the Scotian Shelf from thermal data. Organic maturation studies have been completed by CASSOU *et al.* (1977), POWELL and SNOWDON (1979), PURCELL *et al.* (1979), POWELL (1982) and ISSLER (1984). The only diagenetic studies available are by HERB (1975), which documents diagenetic cements in the Nova Scotia Group sandstones of the Missisauga and Logan Canyon Formations, and NOGUERA URREA (1987), which examines the diagenetic history of over pressure in the Missisauga and Mic Mac Formations. Neither study examines the physicochemical conditions of the mineral reactions observed in the over pressured zone, nor is the relationship between mineral reactions and CO_2 discussed.

The main depositional centre of the Scotian Basin underlies the eastern part of the Scotian Shelf and consists of a wedge of Mesozoic to Cenozoic sediments up to 12 km thick in the vicinity of Sable Island. Triassic and Lower Jurassic redbeds are overlain by Middle Jurassic to Lower Cretaceous deltaic sediments and shelf carbonates. The Verrill Canyon Formation shales are suggested to be the source rock for the gas accumulation at the Venture structure (POWELL, 1982).

Depth relationship of temperature and pressure

Pressures in the Venture area are significantly higher than the hydrostatic pressure ("over pressured"). Fig. 2 shows the variation of pressure and temperature with depth in well B-43 obtained from drill stem test data provided by Mobil Canada. Pressures in this well reach 110 MPa (1100 bars) at 5500 m depth and increase significantly below 4500

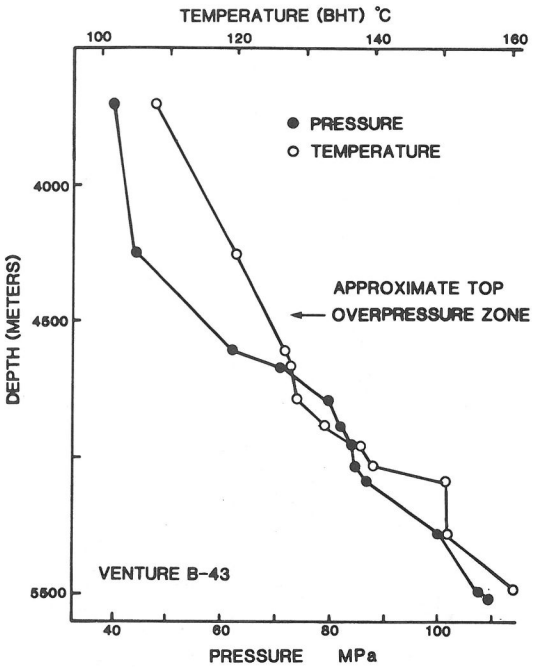

FIG. 2. Depth *vs.* temperature and pressure for well B-43 in the Venture area.

m, the top of the "over pressured" zone. Rock and fluid samples are available over the range from 4000–5500 m and temperatures over this interval, also estimated from drilling data, range from 110 to 160°C. JANSA and NOGUERA URREA (1989) note that the main over pressure zone is in sandstones and that the shales show normal compaction trends and attribute the over pressure to the low geothermal gradient, formation of diagenetic seals, generation of gas and release of water from later stages of shale diagenesis. ISSLER (1984) shows temperatures ranging up to approximately 160°C at 4800 m depth on the Scotian Shelf. Vitrinite reflectance has been measured in samples obtained from wells on the Scotian Shelf by CASSOU *et al.* (1977) and DAVIES and AVERY (1984), who show a marked rate of increase of reflectance with depth in the over pressured zone. The depth to the over pressured zone is variable between wells, but is generally in the range of 4500 m within the Venture area. Over the entire Scotian Shelf the distribution of over pressures is variable.

DIAGENETIC MINERALS, COMPOSITION AND DISTRIBUTION

Observation of the early diagenetic sequence is limited because core samples are available only at deeper intervals. The over pressured zone has been cored in many of the wells in the Venture area and petrographic relationships relevant to the clay-carbonate reaction are described on the basis of samples from these wells.

X-ray diffraction analyses of the less than 2 μm size fraction from sandstones indicates that 14 Å-chlorite is the most abundant clay mineral in the over pressured zone (Fig. 3), ranging up to 98% by weight of the clay size fraction. Above this zone, less than 10% of the clay-size fraction is chlorite; with kaolinite and illite being the most abundant minerals. No expanding clays were observed in the clay-size fraction of the sandstones at these depths. HUTCHEON and NAHNYBIDA (1990) have observed smectite in the shales at depths up to 2300 m and report the details of the analytical procedures used to identify clay minerals in these rocks. The abrupt increase in chlorite content in the over pressured zone can be confirmed by thin section and scanning electron microscope (SEM) examination.

Thin sections were examined in detail but the relevant petrographic features are best summarized by secondary and backscattered electron photomicrographs. Authigenic minerals observed with the SEM include pyrite, quartz overgrowths, illite, kaolinite, chlorite, calcite, ankerite, rutile (?) and sphene. Chlorite is observed lining and filling pores. Quartz overgrowths enclose the pore lining chlorite (Fig. 4a), separating it from the pore filling chlorite. This is interpreted to represent two stages of chlorite

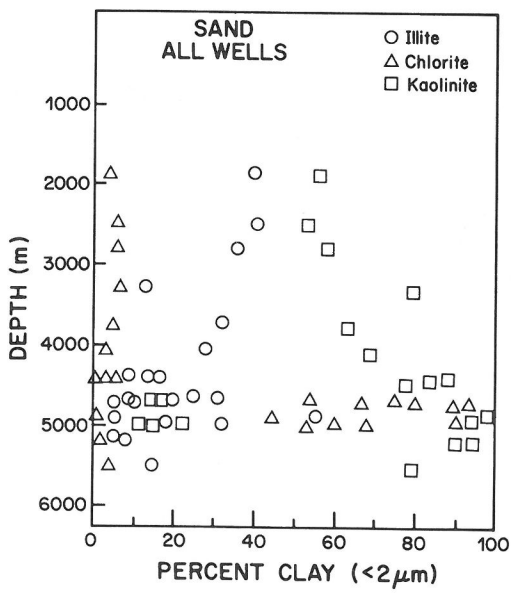

FIG. 3. Clay mineralogy of the less than 2 μm size fraction of sandstones.

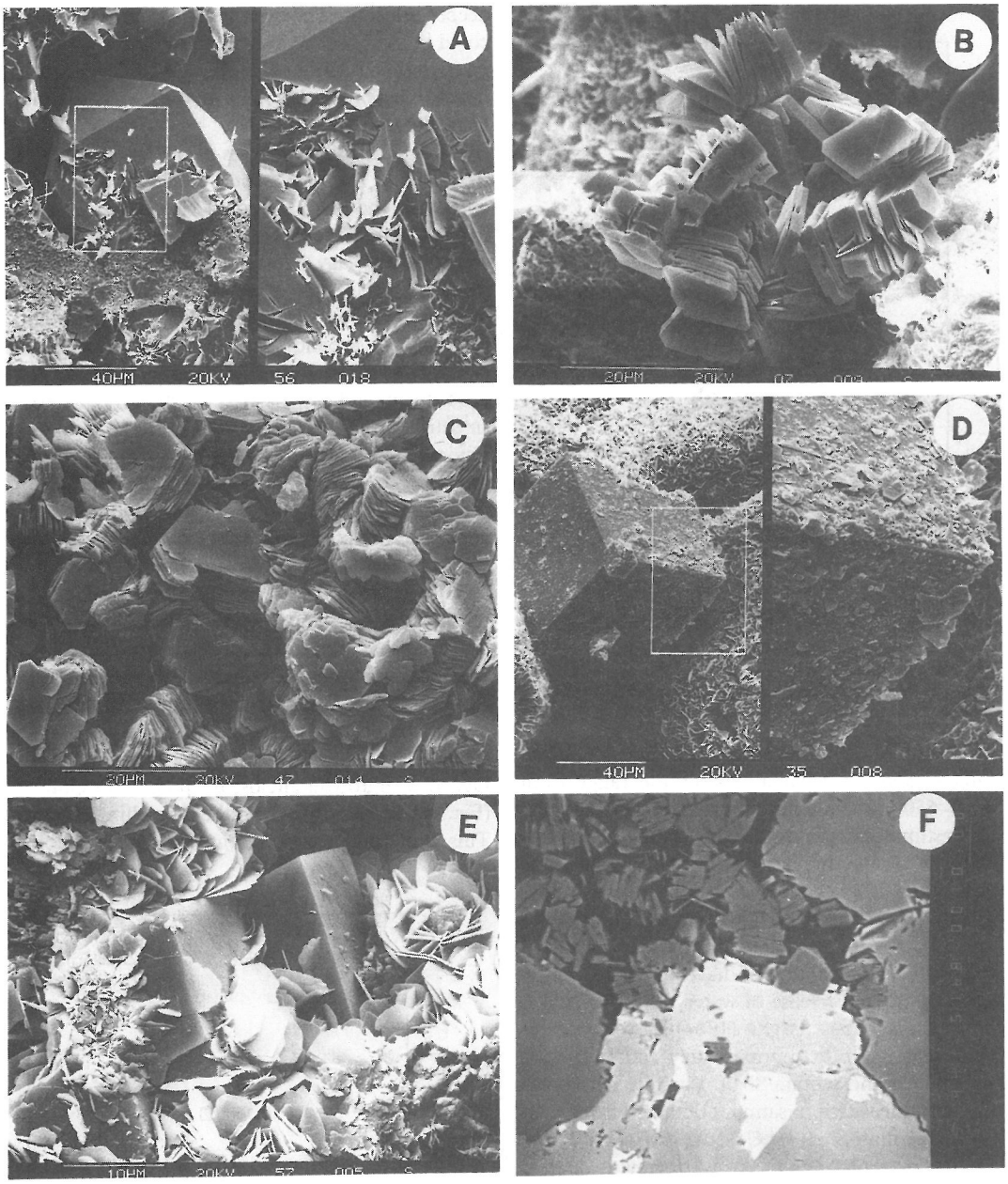

FIG. 4. Petrography of samples examined by scanning electron microscopy. a. Quartz overgrowths enclose pore lining chlorite. The detailed section on the right shows that euhedral quartz has grown over the chlorite rims. The chlorite is interpreted to be an early diagenetic event in this context. (4959 m depth) b. Blocky authigenic kaolinite has well developed crystal faces and the morphology suggests the dickite polytype (4431 m depth). c. Although kaolinite is abundant in some samples, at 4440 m, just above the over pressured zone, the edges of kaolinite crystals are frayed, interpreted to indicate reaction of the kaolinite. d. Fine authigenic chlorite plates coat rhombs of iron calcite at 4955 m depth. This texture is interpreted to be evidence for the chlorite reaction. e. Coarse chlorite rosettes, up to 20 mm, fill pores and are interpreted to be late diagenetic chlorite formed by the clay-carbonate reaction (4959 m depth) f. Backscatter electron micrograph of kaolinite, ankerite and chlorite. Note that ankerite and kaolinite are not observed in contact (4962 m depth).

growth, one early and one later in the paragenetic sequence. At 4430 m, above the over pressured zone in B-43, blocky kaolinite, possibly the dickite variety, (Fig. 4b) is observed. At 4440 m, the kaolinite cleavage flakes are frayed (Fig. 4c), interpreted as possible dissolution of kaolinite. Authigenic pore filling chlorite is present at 4955 m as fine platelets that coat authigenic calcite (Fig. 4d) and at slightly greater depths (4960 m) abundant rosettes of pore filling chlorite are observed (Fig. 4e) to be intergrown with calcite that contains some iron. Ankerite appears above this interval as a replacement of plagioclase feldspar. In the zone with abundant pore-filling chlorite, ankerite is rare. In samples that contain kaolinite, ankerite and chlorite, kaolinite and chlorite are not observed in contact with ankerite (Fig. 4f). These textures are interpreted to indicate a reaction, similar to that documented by HUTCHEON *et al.* (1980), of ankerite and kaolinite to produce calcite and chlorite.

Using the Fe and Mg end-member thermodynamic components, this reaction can be described by the equilibria:

$$5\ CaMg(CO_3)_2 + Al_2Si_2O_5(OH)_4 + SiO_2 + 2\ H_2O \rightleftarrows Mg_5Al_2Si_3O_{10}(OH)_8 + 5\ CaCO_3 + 5\ CO_2 \quad (1)$$

$$5\ FeCO_3 + Al_2Si_2O_5(OH)_4 + SiO_2 + 2\ H_2O \rightleftarrows Fe_5Al_2Si_3O_{10}(OH)_8 + 5\ CO_2. \quad (2)$$

Thermodynamic data are available for all the components in reactions (1) and (2) in HELGESON *et al.* (1978) and WALSHE (1986). Mineral compositions and a model for the dependence of activity on composition are required to examine the phase relationships of reactions (1) and (2) in CO_2-H_2O-NaCl fluids. Compositions of chlorite, calcite and ankerite have been measured by electron microprobe. The compositions measured were used to calculate the activities of the Fe and Mg end-members in chlorite and the activity of $FeCO_3$ in calcite, assuming an ideal solid solution.

Electron microprobe analyses

Mineral compositions were measured on an ARL SEMQ electron microprobe at the University of Calgary using mineral standards of known composition and wavelength dispersive spectrometers. A JOEL 733 electron microprobe at CANMET in Ottawa was also used and analyses were by energy dispersive spectrometer using mineral standards. Points for analyses on the ARL were located by transmitted light optics. In general, operating conditions were 15 kV and 20 nanoamps beam current, although these were varied depending on the stability of the material being analysed. Backscatter electron images, obtained on the JOEL 733, were found to be useful to identify grains suitable for analyses of the fine clay mineral particles. Because the intensity of the backscatter image is proportional to the mean atomic number of the substance under the beam, fine clay plates, with a high mean atomic number and oriented nearly vertically in the low mean atomic number mounting material (epoxy), were relatively easy to recognize from their relative brightness. Although edge effects are a problem with analysis of fine particles, grains as small as a few μm could be analysed and yielded reasonable totals for chlorite (Table 1). The epoxy mounting medium contains no elements common to chlorite and thus the X-rays generated from the epoxy should not substantially affect the analyses.

Composition of chlorite

A number of chlorite grains in various samples were analysed, and the chlorite compositions from wells B-43, B-13, B-52 and J-16 are reported in Table 1. The calculations in this paper are based on the compositions in Table 1. The chlorites are generally iron rich with minor amounts of magnesium, between approximately 3.7 and 6.2 wt.%. There are minor to trace amounts of Na_2O, K_2O, CaO, TiO_2 and MnO. The chlorite grains are relatively homogeneous at the scale of microprobe analyses and the backscatter photomicrographs do not show any bright patches or other indications of inhomogeneous compositions. The observation of fractured samples in reflected electron images shows that some authigenic chlorites have fine fibres of illite growing on them. These might be undetectable using back scatter electrons and could contribute to the K_2O content of the chlorite. Calcite was also observed to be intergrown with chlorite and this may account for the CaO observed in chlorite. Fine grains of authigenic TiO_2, presumably remaining from the destruction of detrital biotite and muscovite, were observed and may account for some of the TiO_2 in the analyses of chlorite and other authigenic phases.

Composition of carbonates

Calcite, siderite, dolomite and ankerite can all be recognized in the samples examined. Ankerite replaces plagioclase feldspar and ranges from 30–50 mol% of the dolomite end-member. Late, pore filling calcite, associated with the pore filling chlorite

Table 1. Chemical compositions (wt.%) of authigenic chlorite in from the Venture Field determined by electron microprobe

Well	Depth (m)	Mineral	No. points	Na_2O	K_2O	CaO	Al_2O_3	SiO_2	TiO_2	FeO	MgO	MnO	SrO	Total*
B-13	4951.0	chlorite	(5)	0.0	0.06	0.0	23.12	26.05	0.0	33.47	6.22	0.09	nd	89.01
B-13	4951.0	calcite	(4)	0.0	nd	54.05	0.0	nd	nd	1.16	0.40	0.79	0.04	56.44
B-13	4956.0	chlorite	(3)	0.0	0.32	0.10	23.97	28.21	0.09	29.85	6.37	0.12	nd	89.03
B-13	4956.0	calcite	(6)	0.0	nd	53.74	0.01	nd	nd	1.07	0.34	0.69	0.04	55.89
B-43	4432.0	ankerite	(5)	nd	nd	31.32	0.0	nd	nd	16.39	8.25	0.97	nd	56.93
B-43	4670.0	ankerite	(4)	nd	nd	31.23	0.0	nd	nd	15.29	8.37	1.33	nd	56.22
B-43	4876.0	ankerite	(3)	nd	nd	31.94	0.0	nd	nd	14.06	9.15	1.10	nd	56.25
B-43	4876.0	calcite	(4)	nd	nd	54.09	0.0	nd	nd	0.80	0.19	0.03	nd	55.11
B-43	4877.0	calcite	(3)	0.10	nd	53.88	0.15	nd	nd	1.21	0.38	0.49	nd	56.21
B-43	4877.0	ankerite	(6)	0.04	nd	30.95	0.11	nd	nd	15.00	8.89	1.27	nd	56.26
B-43	4877.0	chlorite	(3)	0.0	0.11	0.09	23.65	28.97	0.56	30.31	5.69	0.1	nd	89.48
B-43	4956.65	chlorite	(7)	0.0	0.33	0.30	22.99	24.05	0.56	32.15	5.12	0.69	nd	86.19
B-43	4956.65	chlorite	(7)	0.0	0.33	0.30	22.99	24.05	0.56	32.15	5.12	0.69	nd	86.19
B-43	4958.65	chlorite	(18)	0.26	0.08	0.12	22.04	23.71	0.38	33.07	4.84	0.28	nd	84.78
B-43	4958.65	illite	(6)	0.06	9.34	0.12	32.68	49.73	0.21	1.57	0.04	0.56	nd	94.31
B-43	4958.65	albite	(3)	8.72	0.12	0.0	20.23	69.64	0.09	0.16	0.0	0.0	nd	98.96
B-43	4959.	chlorite	(7)	0.02	0.51	0.11	23.93	27.69	nd	30.86	5.76	0.09	nd	89.48
B-43	4959.0	calcite	(4)	0.12	nd	53.63	0.01	nd	nd	0.86	0.50	0.50	nd	55.62
B-43	4432.0	albite	(6)	11.23	0.08	0.82	20.01	67.40	nd	0.04	0.0	nd	nd	99.58
B-43	4670.0	albite	(4)	11.85	0.06	0.03	19.39	67.83	nd	0.18	0.0	nd	nd	99.34
B-43	4876.0	albite	(4)	11.68	0.08	0.08	19.25	68.28	nd	0.03	0.0	nd	nd	99.40
B-43	4958.83	chlorite	(7)	0.0	0.11	0.0	22.5	23.33	0.29	32.65	4.92	0.3	nd	84.10
B-43	4958.83	ankerite	(2)	0.0	0.46	30.51	0.0	0.0	0.0	13.76	9.55	1.38	nd	55.66
B-43	4958.83	albite	(3)	10.10	0.00	0.0	19.24	69.93	0.0	0.0	0.0	0.67	nd	99.94
B-43	4963.0	albite	(6)	11.39	0.26	0.21	19.55	68.73	nd	0.17	0.0	nd	nd	100.31
J-16	5159.0	chlorite	(3)	0.35	0.21	0.20	22.37	21.85	0.25	34.91	4.24	0.29	nd	84.67
J-16	5159.0	ankerite	(3)	0.24	0.39	29.66	0.12	0.33	0.08	17.83	7.11	0.72	nd	56.48
J-16	5159.0	albite	(3)	8.88	0.12	0.08	19.39	70.22	0.18	0.0	0.0	0.0	nd	98.87
J-16	5159.0	siderite	(2)	0.0	0.0	1.95	0.0	0.19	0.0	51.14	7.19	1.76	nd	62.23
J-16	5168.0	chlorite	(13)	0.55	0.25	0.23	23.77	24.46	0.34	36.07	3.66	0.42	nd	89.75
J-16	5168.0	siderite	(6)	0.0	0.0	2.37	0.0	0.91	0.0	49.54	6.68	3.26	nd	62.76
J-16	5168.0	albite	(3)	8.63	0.0	0.12	19.33	72.53	0.21	0.63	0.0	0.0	nd	62.76
B-52	4711.0	chlorite	(2)	0.0	0.15	0.0	13.65	24.78	1.40	35.97	6.20	0.36	nd	82.50
B-52	5125.0	chlorite	(4)	nd	0.34	0.24	25.33	27.53	nd	30.82	4.67	0.07	nd	89.00
B-52	5125.0	ankerite	(5)	0.0	nd	31.02	0.06	nd	nd	15.02	8.61	1.27	0.04	56.02
B-52	5276.26	chlorite	(3)	0.37	0.12	0.0	23.03	23.70	0.27	34.22	4.99	0.38	nd	86.45
B-52	5276.26	calcite	(3)	0.0	0.42	54.44	0.0	0.0	0.0	1.34	0.62	0.32	nd	57.14

* Totals do not include volatiles such as H_2O and CO_2.

and interpreted to be a reaction product, contains approximately 3 to 4 mol% $FeCO_3$. Detrital carbonate grains are variable in abundance in most samples and care was taken during electron microprobe analyses to select only grains that were obviously authigenic. Some spot analyses of detrital calcite grains showed them to have similar compositions to the cement, suggesting that recrystallization of all calcites has taken place. Analyses of selected carbonates are reported in Table 1.

Isotopic compositions

Isotopic compositions of CH_4, CO_2 and calcite were measured in the Stable Isotope Laboratory in the Department of Physics at The University of Calgary. The data collected are presented in Table 2. The compositions of gases in wells O-51, I-93, B-13, B-43, B-52, G-47 and H-22 are from KENDALL *et al.* (1989). Calcite compositions and gas compositions from C-62 and C-74 were measured in this study. The $\delta^{13}C$ of CH_4 ranges from -38 to -45‰ (PDB), reaching the most enriched $\delta^{13}C$ in the over pressured zone (Fig. 5). If the data from each well are observed separately, there is also a tendency for the methane to be more enriched in ^{13}C with depth. The $\delta^{13}C$ values for CO_2 range from -2 to -12‰ (PDB), also reaching the most enriched values in the over pressured zone (Fig. 6). The CO_2 from C-62 and B-52 becomes more enriched with depth, as was observed for methane. A plot of $\delta^{13}CH_4$ *vs.* $\delta^{13}CO_2$ shows the data from all wells

Table 2. Isotopic composition of calcite and CO_2 from the Venture field. The compositions of CO_2 for wells O-51, I-93, B-13, B-43, G-47 and H-22 are from KENDALL *et al.* (1989)

Well	Depth (m)	Temp (°C)	$\delta^{13}CO_2$	$\delta^{13}C$ calcite	Depth (m)	Temp (°C)	$\delta^{13}CO_2$	$\delta^{13}C$ calcite
C-74	3876.5	110	−5.9	−1.56	3876.5	110		−5.05
C-74	3876.5	110		−5.05	3876.5	110		−3.05
C-74	3922	111		−1.35	3922	111		−3.48
C-74	4314.5	121	−6.53	−7.21	4413	123	−3.71	−6.38
C-74	3876.5	110	−5.9	−1.56	3876.5	110		−5.05
C-74	3876.5	110		−3.05	3922	111		−1.35
C-74	3922	111		−3.48	4314.5	121	−6.53	−7.21
C-74	4413	123	−3.71	−6.38	4413		−3.49	
C-74	4514.5	123	−3.12	−4.61	4689.5	130	−3.86	−5.28
C-74	4754.5	131	−2.61	−5.6				
C-62	5021.5	138		17.63	5021.5	138		15.27
C-62	4926.5	136	−10.06	−6.02	4742	131	−12.64	−5.04
C-62	4742		−6.16		4742		−11.62	
O-51	4371	122		−8.48				
I-93	3916	111		−6.67	3928.5	112		2.65
I-93	3998.5	113		−4.12	4086.5	115		−2.69
I-93	4326	121		−0.39				
B-13	4694.7	130		−0.72	4696	130		−1.11
B-13	4699	130		−10.2	4699.5	130		−1.24
B-13	4700	131		−1.1	4700.5	131		−0.94
B-13	4721	131		−4.88	4725.7	131		−9.77
B-13	4727	131		−3.59	4730.9	131		−5.67
B-13	4731	131		−6.75	4732	131		−5.05
B-13	4733	131		−4.49				
B-43	4431	124		−8.85	4435	124		−27.39
B-43	4436	124		−22.5	4437	124		−7.25
B-43	4439	124		−10.73	4440	124		−8.98
B-43	4443	124		−3.26	4670	129		−7.27
B-43	4671	129		−10.23	4676	129		−4.37
B-43	4951	136		−6.3	4966	137		−3.73
B-52	4719	131	−8.51	−5.28	4719	130	−8.51	−4.47
B-52	4967.5		−11.95		5033.5	138	−7.7	−2.91
B-52	5045.5		−7.82		5072.5		−10.21	
B-52	5290	144	−3.86	−3.23	5290	145	−3.86	−4.24
B-52	5290	145	−3.86	−2.43	5728.5		−1.81	
B-52	5802		−3.22					
G-47	4583	127	−5.3	2.79	5230	143	−1.69	1.91
H-22	5022	138	−8.29	−5.27	5022	138	−8.29	−6.21
H-22	5022	138	−8.29	−2.19				
J-16	4869.5	135	−3.56	−1.89	4896.5	135	−3.56	−3.82
J-16	5170	142	−3.92	−0.76	5170	142	−6.52	−3.83

tends to be limited by an $a_c = 1.04$ (Fig. 7) line from WHITICAR *et al.* (1986).

PHASE RELATIONSHIPS OF MINERALS IN H_2O-CO_2-NaCl FLUIDS

The stability of chlorite relative to kaolinite and carbonate (ankerite or dolomite) can be considered by an examination of the phase relationships among these minerals in a CO_2-H_2O-NaCl fluid. Previous studies (TROMMSDORFF and SKIPPEN, 1986) have described the influence of univariant mineral reactions on the compositions of coexisting fluids in metamorphic rocks. They conclude that mineral reactions involving CO_2 and H_2O can buffer the fluid composition to increasing NaCl and CO_2 contents, whereas dehydration reactions tend to buffer the fluid to more H_2O-rich compositions. These conclusions are correct if the dehydration reaction has the "normal" topology in P-T space, that is, the equilibrium temperature increases as water pressure increases. The reaction of kaolinite to illite is interpreted to be important during diagenesis in the Venture area and in other sedimentary basins and can be written as a dehydration reaction. It does, however, have the reverse topology, that is the equilibrium temperature decreases as pressure increases. Reactions of this type also tend to coexist

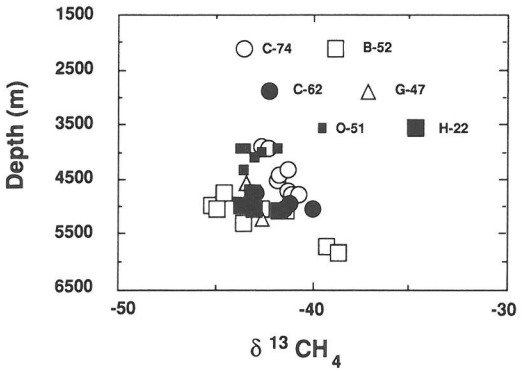

FIG. 5. $\delta^{13}C$ of CH_4 *vs.* depth in meters. Data for wells other than C-62 and C-74 are from KENDALL *et al.* (1989).

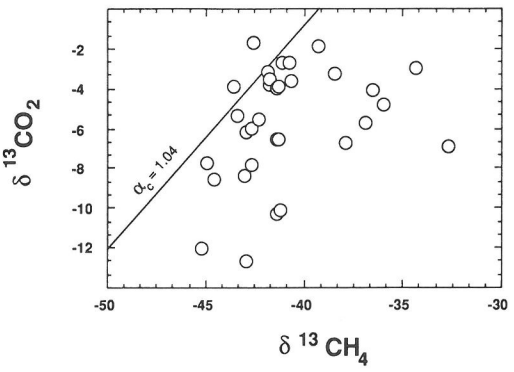

FIG. 7. $\delta^{13}C$ of CO_2 *vs.* $\delta^{13}C$ of CH_4 for all wells with data for both gases. The line labelled $a_c = 1.04$ is from WHITICAR *et al.* (1986).

with a fluid that increases in NaCl and CO_2 with increasing temperature.

Clay-carbonate reactions, specifically with chlorite, have been postulated or described by various authors (ZEN, 1959; MUFFLER and WHITE, 1969; HUTCHEON *et al.*, 1980; MCDOWELL and PACES, 1985) but the mineral compositions required to more accurately determine their stability have not been measured. Further, the phase relationships in a CO_2-H_2O-NaCl fluid, particularly at the limit of CO_2 miscibility in the aqueous phase, have not been determined.

The data used in the following calculations includes the thermodynamic properties of the minerals, mainly from HELGESON *et al.* (1978), with Fe-chlorite data from WALSHE (1986). The solubility of CO_2 in H_2O-NaCl fluids was obtained from BOWERS and HELGESON (1983), ELLIS and GOLDING (1963) and GEHRIG (1980). Using the same methods as HUTCHEON *et al.* (1980), the activity coefficients for mixing of CO_2 and H_2O were obtained on the pseudo-binary at 0, 6 and 20 wt% NaCl using a two-constant Margules mixing model. The activity coefficients for H_2O in the liquid phase and CO_2 in the vapour phase at the conditions of interest were found to be close to unity and not to have a large effect on the calculated stability and have therefore been ignored in the calculations.

The activities of the components in reactions (1) and (2) were calculated using an ideal solution model and the compositions of the appropriate chlorite and carbonate. The stabilities of the reactions are shown on a pseudo-binary T-X_{CO_2} diagram (Fig. 8), at constant pressure, relative to the solubility of CO_2 in 0.0, 6.0 and 20.0 weight percent NaCl solutions. The reaction equilibria that include corrections for the mineral compositions are la-

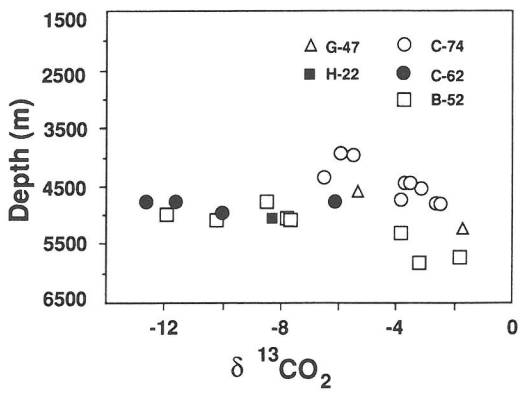

FIG. 6. $\delta^{13}C$ of CO_2 *vs.* depth in meters. Data for from KENDALL *et al.* (1989) were used in addition to data from C-62 and C-74.

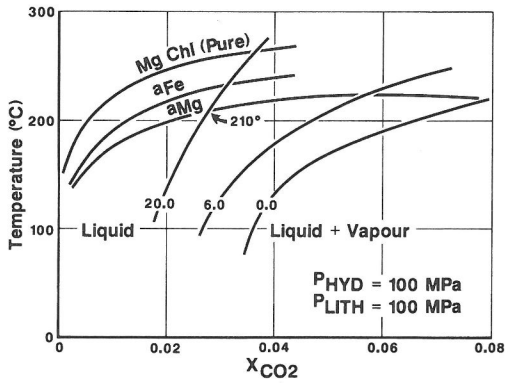

FIG. 8. Stability of Fe- and Mg-chlorite reactions in CO_2-H_2O-NaCl fluid at constant pressure. Note that the intersection of the end member reactions, adjusted for the activities of chlorite and calcite (curves labelled "a_{Mg}" and "a_{Fe}") intersect the 20 weight percent NaCl curve for CO_2 solubility at very similar temperatures.

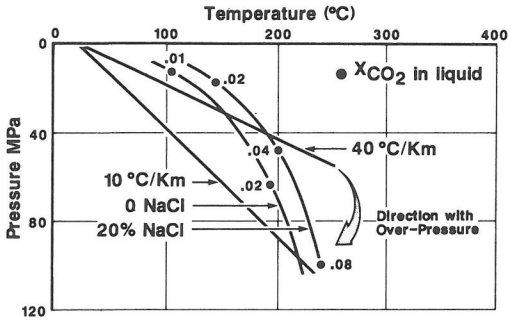

FIG. 9. The trace of the intersections of the kaolinite-carbonate-chlorite reaction with the solubility surface for CO_2 in a CO_2-H_2O-NaCl fluid can be shown as functions of pressure and temperature. The solid lines with the dots are 0 and 20 weight percent NaCl. The numbers beside each dot are the mole fraction of CO_2 in equilibrium at the intersection of the mineral reaction with the CO_2 solubility surface. Note that X_{CO_2}, and thus pCO_2, increases with increasing depth and temperature.

belled on the diagram and intersect the 20 wt% NaCl solubility curve at temperatures between 160 and 170°C, appropriate for a depth of 5000 m or greater in the B-43 well (Fig. 2). Examination of salinities from drill stem tests and interpreted from well logs suggest this is an appropriate salinity for formation waters in the Venture field.

By repeating the calculations at a number of different pressures it is possible to find the temperature of intersections of reactions such as (1) and (2) with the CO_2 solubility surface in a CO_2-H_2O-NaCl fluid. These can then be presented as a *P-T* diagram with the locus of the intersections for various NaCl contents and the mole fraction of CO_2 noted along the trace of the intersection. Fig. 9 shows such a diagram and a number of features are evident upon examination. Firstly, the evolution of a fluid coexisting with the reactions as written has the appropriate sense of compositional evolution. That is, the fluid becomes enriched in NaCl and CO_2 with increasing temperature and pressure. This does not imply that the solubility of CO_2 increases with increasing NaCl content because the pressure is also increasing. Over the range of pressures, temperatures and NaCl contents examined here it is apparent that increases in pressure increase the solubility of CO_2 and are sufficient to overcome the decrease in CO_2 solubility imposed by higher NaCl contents. Superimposed on the diagram are geothermal gradients for 10 and 40°C/km. The trace of the intersection between the CO_2 solubility surface and the mineral reaction first intersects the geothermal gradient at a temperature of about 140–150°C for a solution with 0.0 wt% NaCl. This is the minimum temperature at which the kaolinite-carbonate to calcite reaction will be in equilibrium on the CO_2 solubility surface.

Using the fractionation factors for ^{13}C between CO_2 and calcite and temperature estimates, it is possible to calculate the expected isotopic composition of CO_2 from the measured calcite composition and compare it to the measured CO_2 composition. Temperature at various depths has been measured by Mobil Oil for the wells in this study. The isotopic compositions of calcite was determined as part of this study and the isotopic compositions for CO_2 in the gas that were not available from KENDALL *et al.* (1989) were measured, if samples were available. The results of these calculations are shown in Fig. 10. Some of the points are not in good agreement with the predicted value expected if the calcite were in isotopic equilibrium with CO_2 in the gas. Some of these samples, shown as shaded points in Fig. 10, have considerable amounts of detrital carbonate.

BUFFERING

The calculation of the stability of clay-carbonate reactions does not define the reaction mechanism that produces the CO_2 observed in sedimentary basins. It is possible that other reactions, such as those involving smectite (GUNTER and BIRD, 1988) or illite (HUTCHEON *et al.*, 1980) and mixed volatiles would be stable at lower temperatures at the same pressure, and intersect the solubility surface of CO_2 in H_2O-CO_2-NaCl mixtures at lower temperatures. Reactions involving smectite or illite may be candidates to produce CO_2 by calcite dissolution during the diagenesis of shales.

MCDOWELL and PACES (1985) note that reaction among silicates and carbonates takes place in an

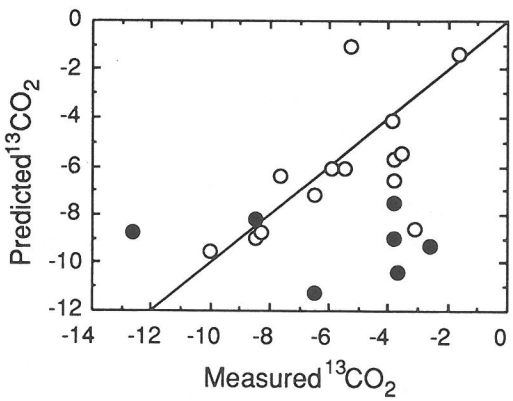

FIG. 10. The comparison of measured and expected compositions of CO_2. The shaded symbols represent samples with primarily detrital carbonate.

aqueous liquid and involves aqueous ions such as HCO_3^- and Ca^{2+}. Without measured concentrations of ions in solution it is not possible to calculate the stability of such reactions in a CO_2-H_2O-NaCl fluid. Once the aqueous phase is saturated with CO_2, further dissolution of carbonate will produce CO_2 directly into the vapour phase. Consideration of different reactions raises the question of how carbonates are dissolved and thus the question of how pH is buffered during diagenesis. SURDAM *et al.* (1989) have suggested that the organic acids are the most effective pH buffers over a considerable range of diagenetic temperatures. LUNDEGARD and LAND (1989) have examined the carbonate equilibria in the presence of organic acids and changing pCO_2. ABERCROMBIE (1989) examined buffering capacities for the carbonate minerals, dissolved carbonate and silicate minerals and found that hydrolysis of silicates has the greatest buffer capacity. His calculations did not consider aqueous organic species. HUTCHEON and ABERCROMBIE (1989a) show that, for most of the pH range, acetate solutions of 3000 mg/l have lower buffering capacity than a reaction between albite and smectite. GUNTER and BIRD (1988) have observed the production of CO_2 during hydrothermal experiments and suggest that silicate hydrolysis reactions are the source of protons for calcite dissolution. HUTCHEON and ABERCROMBIE (1989a,b) also present evidence from field data that aluminous silicates, such as kaolinite, function as "acids" as temperature increases during diagenesis. They show that the Na^+/H^+ and K^+/H^+ activity ratios of the fluids are in metastable equilibrium with silicate minerals observed in thermal flooding of heavy oil reservoirs, but that the $Ca^{2+}/(H^+)^2$ activity ratio was determined by calcite dissolution.

SMITH and EHRENBERG (1989) show a trend of temperature and pCO_2 for the Gulf Coast and North Sea and suggest the trend may be the result of hydrolysis reactions among silicates causing dissolution of carbonates. ARNÓRSSON *et al.* (1983a,b) have studied the compositions of fluids from geothermal wells and springs in Iceland and show fluid saturation with respect to silicates such as albite, smectite and analcime. They report a similar trend of pCO_2 *vs.* temperature for geothermal wells in basaltic rocks from Iceland. HUTCHEON and ABERCROMBIE (1989a) note that the data of ARNÓRSSON *et al.* (1983b) show a lower pCO_2 at any particular temperature than the data shown by SMITH and EHRENBERG (1989) for sedimentary rocks from the Gulf Coast.

The dissolution of calcite in an aqueous solution saturated with CO_2 can be described by the equilibrium:

$$CaCO_3 + 2H^+ \rightleftarrows Ca^{2+} + H_2O + CO_2. \quad (3)$$

At equilibrium, a higher imposed aH^+ (lower pH) would require a higher pCO_2 to maintain equilibrium with calcite. The trend of lower pCO_2 values at any temperature for the geothermal fluids from Iceland suggests that potential silicate hydrolysis reactions buffering pH are more "basic" than those of the Gulf Coast. ABERCROMBIE (1988) and HUTCHEON and ABERCROMBIE (1989b) have concluded from samples of hot fluids recovered from volcaniclastic rocks that these rocks are in metastable equilibrium with analcime and smectite. HUTCHEON *et al.* (1988) sampled waters from quartz-rich reservoirs and volcaniclastic reservoirs and determined that the fluids in quartz rich reservoirs were more "acidic" and in metastable equilibrium with kaolinite-smectite and the fluids from the volcaniclastic reservoirs were more "basic" and in equilibrium with smectite-analcime. Examination of the phase relationships for Na-Al-Si-O-H minerals shows that, in general, the smectite-analcime reaction is stable at values of Na^+/H^+ activity approximately two orders of magnitude (depending on temperature) higher than the kaolinite-smectite reaction. At similar Na^+ activities, the Na^+/H^+ activity ratio can only change significantly by changes in aH^+.

The calcite dissolution reaction (3), as written above, has a value of pCO_2 that depends on the activity of Ca^{2+} and H^+ in solution. Typically activities of H^+ will be 10^{-5} to 10^{-7} and the activity of Ca^{2+} will be approximately 10^{-2}, or three to five orders of magnitude greater. For reaction (3) the equilibrium constant is:

$$K = \frac{[aCa^{2+}][fCO_2]}{[aH^+]^2}.$$

Inspection of the equilibrium constant indicates that very small changes in aH^+, which is a squared term and a very small number compared to aCa^{2+}, will cause relatively large changes in fCO_2. For example, a one order of magnitude change in aH^+ will be reflected by a two order of magnitude change in log fCO_2 and, therefore, in log pCO_2. Fig. 11 shows the temperature-pCO_2 trends for fluids from sediments of the Gulf Coast (SMITH and EHRENBERG, 1989) and fluids from geothermal wells in basaltic rocks from Iceland (ARNÓRSSON *et al.*, 1983b). The Gulf Coast rocks would be expected to have more acidic pH (higher aH^+) values imposed by reactions among kaolinite and smectite or illite, whereas the

Icelandic fluids would (for similar $a\mathrm{Na}^+$) be expected to have more basic pH (lower $a\mathrm{H}^+$) imposed by equilibria between smectite, analcime and albite.

Rocks in the Gulf Coast are reported to contain kaolinite and calcite as authigenic phases. To test the proposition that CO_2 partial pressures are determined by calcite dissolution regulated by silicate hydrolysis, water analyses were selected from the Gulf Coast (KHARAKA *et al.*, 1985) and Iceland (ARNÓRSSON *et al.*, 1983a). The analyses from the Gulf Coast were processed using EQ3 (WOLERY, 1983) with the conditions that the activity of Al^{3+} be set by equilibrium with kaolinite, $a\mathrm{H}^+$ be set by equilibrium with illite and $a\mathrm{HCO}_3^-$ be set by calcite. Illite was included in the calculations as muscovite and the resulting $p\mathrm{CO}_2$ adjusted by considering the activity of muscovite in illite to be 0.1. The effect of varying muscovite activity in illite from 1.0 to 0.1 has a minimal effect on the calculations. The program was executed at temperatures between 25 and 250°C under these conditions, providing calculated values for the fugacity of CO_2. The calculated fugacity of CO_2 was used with fugacity coefficients (ANGUS *et al.*, 1976), assuming a geothermal gradient of 30°C/km and a fluid pressure gradient of 105 bars per kilometer, to determine the value of $p\mathrm{CO}_2$ at each temperature. These values were plotted as a line on Fig. 11 that is in reasonable agreement with the data points measured by SMITH and EHRENBERG (1989). EQ3 calculates high temperature aqueous reactions for pressures determined by the boiling curve for pure water and clearly the formation waters of the Gulf Coast have high salinities. The partial pressure of CO_2 has been calculated only from equilibrium with calcite and all other variables are essentially imposed by the mineral assemblage chosen, thus the salinity effect should not be significant.

Attempts to saturate different water analyses from Iceland with smectite, calcite and albite were only successful up to 200°C (Fig. 11). Above this temperature EQ3 failed to execute successfully. The thermodynamic data for smectite and analcime are probably not of as good quality as the other data in the EQ3 data base and this may explain the lack of success in achieving numerical solutions to the problem. The data of ARNÓRSSON *et al.* (1983a,b) show that in the rocks they examined there are two different mineral assemblages, smectite-albite below 200°C and chlorite-epidote without smectite above 200°C. Fig. 11 shows a break in the trend of $p\mathrm{CO}_2$ *vs.* temperature at approximately 200°C that may be related to this change in mineral assemblages. The data in Fig. 10 was used to calculate the trend of log $p\mathrm{CO}_2$ *vs.* temperature for the kaolinite-carbonate-chlorite reaction in the Venture Field. The line passes through the higher temperature data reported by ARNÓRSSON *et al.* (1983b) in the temperature range reported for stable chlorite in the rocks from Iceland.

The trend of temperature with $p\mathrm{CO}_2$ can be explained for both sets of data by considering schematically the change in position of the intersection of reaction (3) with limit of miscibility of CO_2 in a H_2O-NaCl aqueous solution (Fig. 12). At P_1 the intersection of the mineral reaction and the CO_2

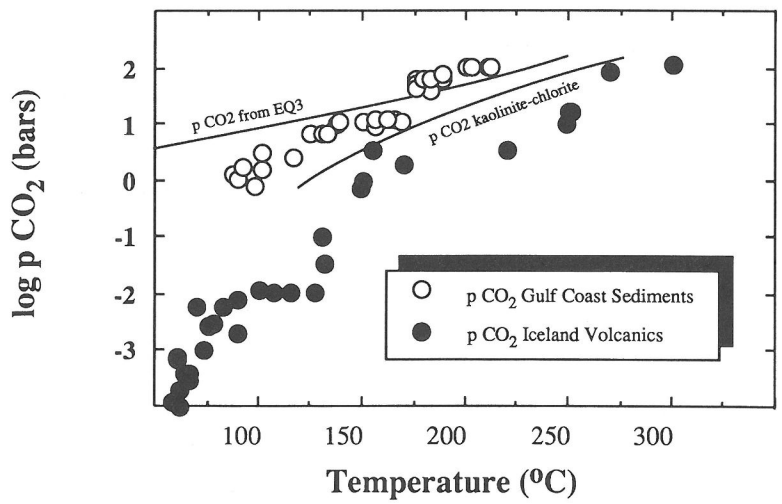

FIG. 11. Temperature-$p\mathrm{CO}_2$ trends from Iceland and Gulf Coast. The line that passes through the Gulf Coast data was calculated using EQ3 and assuming equilibrium between the fluid, calcite, kaolinite, illite and CO_2.

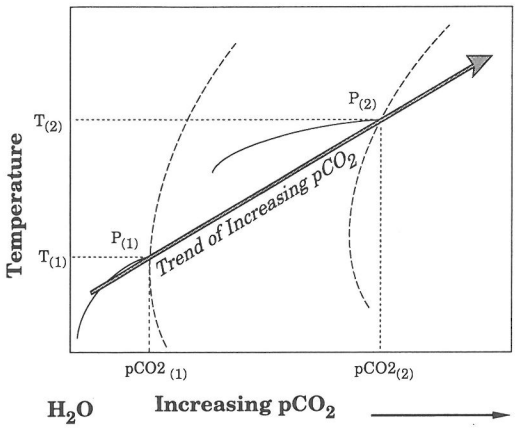

FIG. 12. Schematic representation of intersections of mineral reactions with the CO_2 solubility surface as a function of pCO_2 and temperature at two pressures, P_1 and P_2.

solubility surface is at a particular temperature, T_1. At some higher pressure, P_2, the solubility of CO_2 in the aqueous phase will be higher and there will be a point of intersection of reaction (3) at some higher temperature, T_2. If aH^+ is buffered by a relatively "acidic" assemblage, such as kaolinite-illite, the corresponding pCO_2 at any temperature will be higher than if aH^+ is buffered by a relatively "basic" mineral assemblage such as illite-K-feldspar or smectite-albite. It is likely that the locus of intersections of the mineral reactions with the solubility surface for most silicate hydrolysis reactions in rocks containing calcite (or other carbonates) will produce a relatively linear trend of temperature *vs.* $\log pCO_2$. Fig. 12 also describes graphically the method used to calculate the position of the intersection between the chlorite-kaolinite reaction and the miscibility surface for CO_2 as shown in Fig. 9.

CONCLUSIONS

The authigenic mineral assemblages of the sandstones in the Venture Field show textural and petrographic evidence that clay-carbonate reactions involving kaolinite, ankerite chlorite and calcite probably have taken place. Analysis of mineral compositions and the application of the composition, with thermodynamic data and the solubility of CO_2 in H_2O-NaCl aqueous fluids shows that equilibria (1) and (2) can be used to determine that equilibrium temperatures for the clay-carbonate reaction are about 160°C, which is near the upper limit of reasonable temperatures for the over pressured zone of the Venture Field. The isotopic composition of calcite and CO_2 is consistent with an origin for the CO_2 from a clay-carbonate reaction.

The metastable equilibrium stability of chlorite, kaolinite and carbonates does not shed any light on the reaction mechanism. The suggestion that silicate hydrolysis controls the pH of the aqueous phase has been tested by considering the compositions of waters, buffered by silicate hydrolysis reactions, and calculating the values of pCO_2 that would result at any temperature. The calculated pCO_2 agrees reasonably well with measured trends for fluids from quartzose sedimentary rocks from the Gulf Coast and less well with geothermal fluids from basaltic volcanic rocks in Iceland suggesting that the trends of pCO_2 observed in sedimentary basins and hydrothermal fluids at temperatures in the range of 300°C, or lower, are controlled by silicate-carbonate mineral reactions.

Acknowledgements—This work was completed while the author was on a Senior Industrial Fellowship sponsored by NSERC (The Natural Sciences and Engineering Research Council, Canada), Shell Canada Limited and The University of Calgary. I am in debt to all three organizations for their support. Most of the data were collected with the cooperation of Mobil Oil Canada over an extended period between 1982 and 1986. Jo van Elsberg, Catherine Chaplin and Dave Blair, all formerly of Mobil, among many others at Mobil Oil Canada, were extremely helpful and cooperative with sampling core, interpreting data and providing moral support and discussions. The isotopic analyses were done in the Physics Department in the NSERC supported laboratory of H. R. Krouse at The University of Calgary and I am, as always, grateful for their assistance. Cynthia Nahnybida and Steve Machemer did some of the electron microprobe analyses, the remainder were done by the author under the guidance of Paul Mainwaring of CANMET, whose patience with probe initiations is legendary. Discussions with Hugh Abercrombie, Glenn Wilson and Steve Ehrenberg have been very helpful. The assistance of Ritsue Imakiire and Bill Bourcier in getting EQ3/6 running was much appreciated. Critical comments by John Bloch improved the final manuscript. Financial support for this project was received from Mobil Canada, a research contract with the Geological Survey of Canada and NSERC.

REFERENCES

ABERCROMBIE H. J. (1988) Water-rock interaction during diagnesis and thermal recovery, Cold Lake, Alberta. Unpublished Ph.D. Thesis. The University of Calgary, Calgary, Alberta.

ANGUS S., ARMSTRONG B. and DE RUECK K. (1976) International Thermodynamic Tables of the Fluid State Carbon Dioxide, Vol. 3. Pergamon Press.

ARNÓRSSON S., GUNNLAUGSSON E. and SVAVARSSON H. (1983a) The chemistry of geothermal waters in Iceland. II. Mineral equilibria and independent variables controlling water compositions. *Geochim. Cosmochim. Acta* **47**, 547–566.

ARNÓRSSON S., GUNNLAUGSSON E. and SVAVARSSON H.

(1983b) The chemistry of geothermal waters in Iceland. III. Chemical geothermometry in geothermal investigations. *Geochim. Cosmochim. Acta* **47,** 567–577.

BOWERS T. S. and HELGESON H. C. (1983) Calculation of thermodynamic and geochemical consequences of nonideal mixing in the system H_2O-CO_2-NaCl on phase relations in geologic systems: Equation of state for H_2O-CO_2-NaCl fluids at high pressures and temperatures. *Geochim. Cosmochim. Acta* **47,** 1247–1275.

CASSOU A., CONNAN J. and PORTHAULT B. (1977) Relations between maturation of organic matter and geothermal effect, as exemplified in Canadian east coast offshore wells. *Bull. Canadian Petrol. Geol.* **25,** 174–194.

DAVIES E. H. and AVERY M. P. (1984) A system for vitrinite reflectance analysis on dispersed organic matter for offshore Eastern Canada. *Geol. Surv. Canada Paper* 84-1A, 367–372.

ELLIS A. J. and GOLDING R. M. (1963) The solubility of carbon dioxide above 100°C in water and in sodium chloride solutions. *Amer. J. Sci.* **261,** 47–60.

GEHRIG M. (1980) Phasengleichgewichte und PVT-Daten ternarer Mishungen aus Wasser, Kohlendioxid und Natriumchlorid bis 3 Kbar und 550C. Unpublished Ph.D. Dissertation. Karlsruhe University, Germany.

GIVEN M. M. (1977) Mesozoic and early Cenozoic geology of offshore Nova Scotia. *Bull. Canadian Petrol. Geol.* **25,** 63–91.

GRADSTEIN F. M., WILLIAMS G. L., JENKINS W. A. M. and ASCOLI P. (1975) Mesozoic and Cenozoic stratigraphy of the Atlantic continental margin, Eastern Canada. *Canadian Soc. Petrol. Geol. Mem.* **4,** 103–131.

GUNTER W. G. and BIRD G. W. (1988) CO_2 production in tar sand reservoirs under in situ steam temperatures: reactive calcite dissolution. *Chem. Geol.* **70,** 301–311.

HAWORTH R. T. (1975) The development of Atlantic Canada as a result of continental collision—evidence from offshore gravity and magnetic data. *Canadian Soc. Petrol. Geol. Mem.* **4,** 59–77.

HELGESON H. C., DELANY J. M., NESBITT H. W. and BIRD D. K. (1978) Summary and critique of the thermodynamic properties of rock-forming minerals. *Amer. J. Sci.* **278A,** 1–229.

HERB G. (1975) Diagenesis of deeply buried sandstones on the Scotian Shelf. Ph.D. Thesis. Dalhousie University, Dartmouth, Nova Scotia.

HOWIE R. D. and BARSS M. S. (1975) Paleogeography and sedimentation in the upper Paleozoic, Eastern Canada. *Canadian Soc. Petrol. Geol. Mem.* **4,** 45–57.

HUTCHEON I. and NAHNYBIDA C. G. (1990) Clay mineralogy and diagenesis of sandstones and shales from the Venture Region, Nova Scotia, Canada. (in preparation).

HUTCHEON I., ABERCROMBIE H. and KROUSE H. R. (1990) Inorganic origin of carbon dioxide production in low temperature thermal recovery of bitumen: Chemical and isotopic evidence. *Geochim. Cosmochim. Acta* (in press).

HUTCHEON I. and ABERCROMBIE H. (1989a) Carbon dioxide in clastic rocks and silicate hydrolysis. *Geology* (submitted).

HUTCHEON I. and ABERCROMBIE H. (1989b) Fluid-rock interactions in thermal recovery of bitumen, Tucker Lake Pilot, Cold Lake, Alberta. *Amer. Assoc. Petrol. Geol.* Special volume on reservoir prediction (submitted).

HUTCHEON I., ABERCROMBIE H., SHEVALIER M. and NAHNYBIDA C. (1988) A comparison of formation reactivity in quartz-rich and quartz-poor reservoirs during steam assisted recovery. *Fourth International UNITAR/UNDP Conference on Heavy Crude and Tar Sands.* Paper 235. Edmonton.

HUTCHEON I., OLDERSHAW A. and GHENT E. (1980) Diagenesis of Cretaceous sandstones of the Kootenay Formation at Elk Valley (southeastern British Columbia) and Mt. Allan (southwestern Alberta). *Geochim. Cosmochim. Acta* **44,** 1425–1435.

ISSLER D. R. (1984) Calculation of organic maturation levels for offshore eastern Canada,—Implications for general application of Lopatin's method. *Canadian J. Earth Sci.* **21,** 477–488.

JANSA L. F. and WADE J. A. (1975) Paleogeography and sedimentation in the Mesozoic and Cenozoic, southeastern Canada. *Canadian Soc. Petrol. Geol. Mem.* **4,** 103–131.

JANSA L. F. and NOGUERA URREA V. H. (1989) Geology and genesis of over pressured sandstone reservoirs in the Venture gas field, Offshore Nova Scotia, Canada (abstr.). *Annual Convention Amer. Assoc. Petrol. Geol.,* San Antonio, Texas.

KEEN C. E. (1979) Thermal history and subsidence of rifted continental margins—evidence from wells on the Nova Scotia and Labrador shelves. *Canadian J. Earth Sci.* **16,** 505–522.

KEEN C. E. (1983) Salt diapirs and thermal maturity: Scotian Basin. *Bull. Canadian Petrol. Geol.* **31,** 101–108.

KEEN C. E. and LEWIS T. (1982) Measured radiometric heat production in sediments from the continental margin of eastern North America: Implications for petroleum generation. *Bull. Amer. Assoc. Petrol. Geol.* **66,** 1402–1407.

KENDALL S., KROUSE H. R. and ALTEBAUEMER F. (1989) Isotopic evidence for the generation and migration of gas, Sable sub-basin, Scotian Shelf, Canada. *Bull. Canadian Petrol. Geol.* (submitted).

KHARAKA Y. K., HULL R. W. and CAROTHERS W. W. (1985) Water-rock interactions in sedimentary basins. In *Relationship of Organic Matter and Mineral Diagenesis* (ed. D. L. GAUTIER). Soc. Econ. Paleontol. Mineral. Short Course 17.

LUNDEGARD P. D., LAND L. S. and GALLOWAY W. E. (1984) Problem of secondary porosity: Frio Formation (Oligocene), Texas Gulf Coast. *Geology* **12,** 399–402.

LUNDEGARD P. D. and LAND L. S. (1986) Carbon dioxide and organic acids: their role in porosity enhancement and diagenesis of the Texas Gulf Coast. *Soc. Econ. Paleontol. Mineral. Spec. Publ.* **38,** 129–146.

LUNDEGARD P. D. and LAND L. S. (1989) Carbonate equilibria and pH buffering by organic acids—response to changes in pCO_2. *Chem. Geol.* **74,** 277–287.

MCDOWELL S. D. and PACES J. B. (1985) Carbonate alteration minerals in the Salton Sea geothermal system, California, USA. *Mineral. Mag.* **49,** 469–479.

MCIVER N. L. (1972) Cenozoic and Mesozoic stratigraphy of the Nova Scotia shelf, *Canadian J. Earth Sci.* **9,** 54–69.

MUFFLER L. P. J. and WHITE D. E. (1969) Active metamorphism of Upper Cenozoic sediments in the Salton Sea geothermal field and the Salton Trough, Southeastern California. *Bull. Geol. Soc. Amer.* **80,** 157–182.

NOGUERA URREA V. H. (1987) Geology and diagenetic history of over pressured reservoirs in the lower Mississauga-Mic Mac Formations of the Venture gas field,

Scotian Shelf, Nova Scotia. Unpublished M.Sc. Thesis. Dalhousie University, Dartmouth, Nova Scotia.

PARSONS M. G. (1975) The geology of the Laurentian fan and the Scotian rise. *Canadian Soc. Petrol. Geol. Mem.* **4,** 155–167.

PIPER D. J. W. (1975) Late quaternary deep water sedimentation off Nova Scotia and western Grand banks. *Canadian Soc. Petrol. Geol. Mem.* **4,** 195–204.

POWELL T. G. and SNOWDON L. R. (1979) Geochemistry of crude oils and condensates from the Scotian Basin, offshore eastern Canada. *Bull. Canadian Petrol. Geol.* **27,** 453–466.

POWELL T. G. (1982) Petroleum geochemistry of the Verrill Canyon formation: a source for Scotian shelf hydrocarbons. *Bull. Canadian Petrol. Geol.* **30,** 167–179.

PURCELL L. P., RASHID M. A. and HARDY I. A. (1979) Geochemical characteristics of sedimentary rocks in the Scotian Basin. *Bull. Amer. Assoc. Petrol. Geol.* **63,** 87–105.

SMITH H. A. (1975) Geology of the West Sable structure. *Bull. Canadian Petrol. Geol.* **23,** 109–130.

SMITH J. T. and EHRENBERG S. N. (1989) Correlation of carbon dioxide abundance with temperature in clastic hydrocarbon reservoirs: Relationship to inorganic chemical equilibrium. *Marine Petrol. Geol.* **6,** 129–135.

SURDAM R. C., CROSSEY L. G., HAGEN E. S. and HEASLER H. P. (1989) Organic-inorganic interactions and sandstone diagenesis. *Bull. Amer. Assoc. Petrol. Geol.* **73,** 1–23.

SWIFT J. H., SWITZER R. W. and TURNBULL W. F. (1975) The Cretaceous Petrel Limestone of the Grand Banks, Newfoundland. *Canadian Soc. Petrol. Geol. Mem.* **4,** 181–194.

TROMMSDORFF V. and SKIPPEN G. B. (1986) Vapour loss ("boiling") as a mechanism for fluid evolution in metamorphic rocks. *Contrib. Mineral. Petrol.* **94,** 317–322.

WALSHE J. L. (1986) A six-component chlorite solid solution model and the conditions of chlorite formation in hydrothermal and geothermal systems. *Econ. Geol.* **81,** 681–703.

WHITICAR M. J., FABER E. and SCHOELL M. (1986) Biogenic methane formation in marine and freshwater environments: CO_2 reduction *vs.* acetate fermentation—Isotope evidence. *Geochim. Cosmochim. Acta* **50,** 693–709.

WOLERY T. J. (1983) EQ3NR A program for geochemical aqueous speciation-solubility calculations: User's guide and documentation. Lawrence Livermore Laboratory Report UCRL-53414.

ZEN E-AN (1959) Clay mineral-carbonate relations in sedimentary rocks. *Amer. J. Sci.* **257,** 29–43.